Electronic Supplementary Material (ESI) for RSC Advances.
This journal is © The Royal Society of Chemistry 2015

Structure and Oxide ion Conductivity in Tetragonal Tungsten Bronze $BaBiNb_5O_{15}$

HongqiangMa[a], Kun Lin[a], LonglongFan[a], YangchunRong[a], Jun Chen[a] , JinxiaDeng[ab],

LaijunLiu[c]， Shogo Kawaguchi[d], Kenichi Kato[e], Xianran Xing*[,a]

[a] *Department of Physical Chemistry,* [b]*Department of Chemistry, University of Science and Technology Beijing, Beijing 100083, China*

[c] *State Key Laboratory Breeding Base of Nonferrous Metals and Specific Materials Processing, Guilin University of Technology, Giulin 541004, China*

[d]*Japan Synchrotron Radiation Research Institute (JASRI)1-1-1, Kouto, Sayo-cho, Sayo-gun, Hyogo 679-5198, Japan*

[e]*RIKEN SPring-8 CenterSayo, Hyogo 679-5148, Japan*

Corresponding author

Department of Physical Chemistry, University of Science and Technology Beijing, Beijing 100083, China

Tel: +86-10-62334200

Fax: +86-10-62332525

*e-mail address: xing@ustb.edu.cn

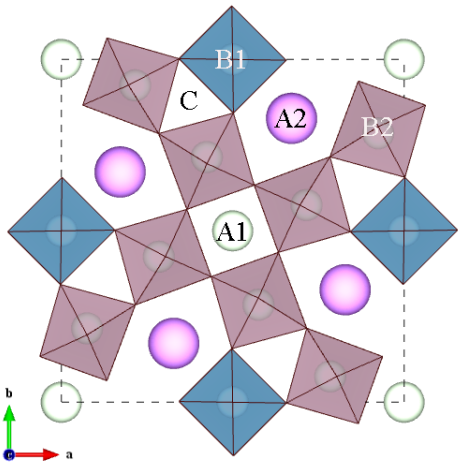

Fig. S1 Schematic representation of the structural skeleton of the TTB-type structure view along [001], which shows atoms in A sites and NbO_6 octahedra.

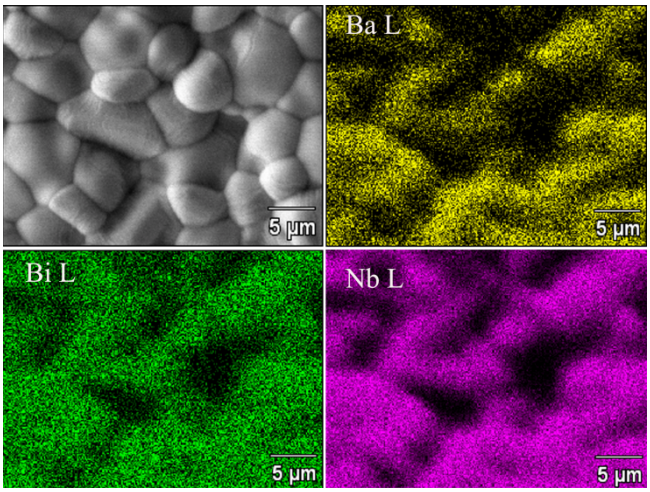

Fig. S2 SEM image and the corresponding element distributions of selected surface of a pellets of BBN sintered at 1240°C for 2 h.

The sintering conditions for the BBN ceramics led to 95% of relative density value for the specimens. The microstructures and element distributions were studied using a scanning electron microscopy (SEM, Supra 55; Zeiss, Oberkochen, Germany) coupled with energy dispersive X-ray spectroscopy (EDS). It shows the grain size is about 6 ~ 15 µm and the cationic elements (Ba, Bi, Nb) are uniformly distributed.

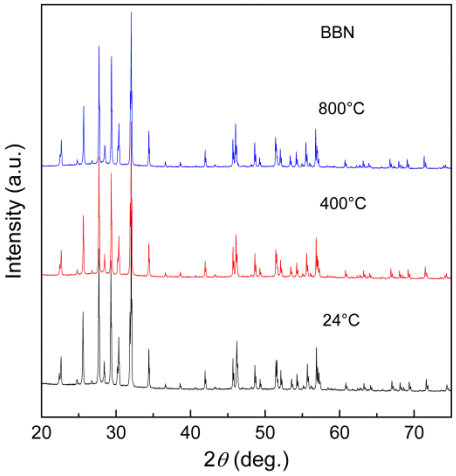

Fig. S3 XRD patterns of BBN powder at different temperatures, indicating no phase transition occurs in the measured temperature.

The high-temperature powder X-ray diffraction patterns were collected on a laboratory diffractometer, (PANalytical X' Pert^{III}, Holland, Cu Kα, λ=1.5406 Å) and an Anton Paar HTK 1200 high-temperature attachment was used. Data were collected at RT, 400, 800°C over a 2θ range of 8 to 120° in 0.0131° steps. The heating rate was 10°C/min, and the sample was held for 15 min at a specified temperature to reach heating equilibrium.

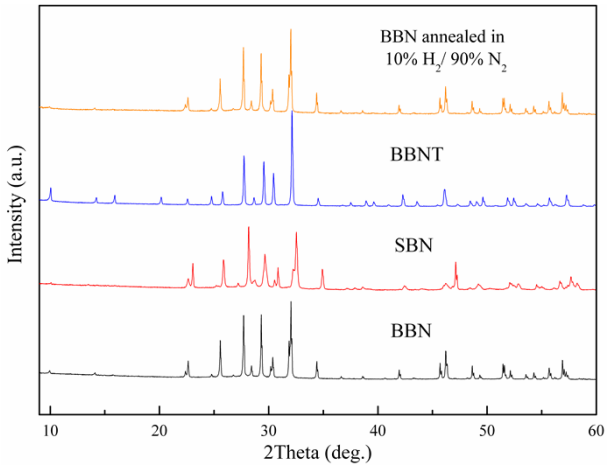

Fig. S4 XRD patterns of as made BBN, SBN, and BBNT samples. All these samples are indexed as TTB. Actually, BBN and SBN are unfilled TTB, and BBNT is filled TTB. The powder XRD of the sintered pellet of BBN annealed at 800 °C for 6 h at 5%H_2 / 5%N_2 atmosphere are also shown, There is almost no change of all the peaks in XRD pattern, suggesting that it is structurally stable in the reducing conditions.

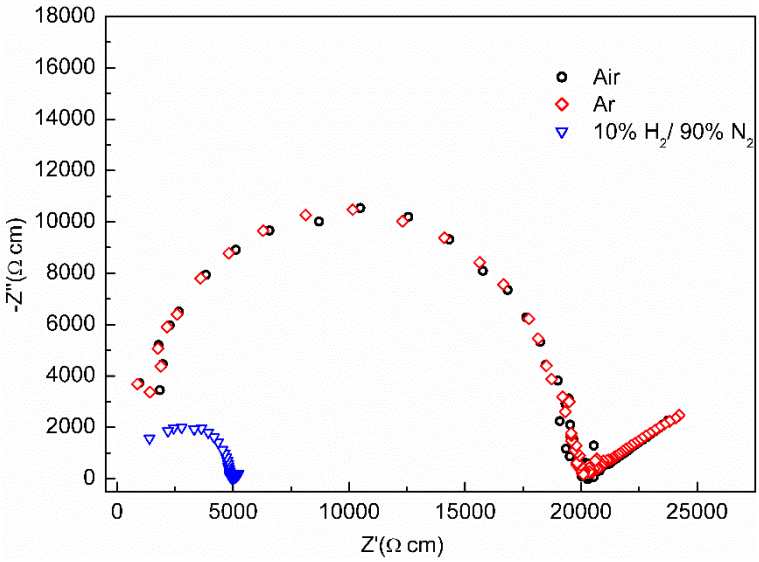

Fig. S5 Complex impedance plots for the BBN measured at 550°C in air, Ar gas and 10%H_2/90%N_2, respectively.

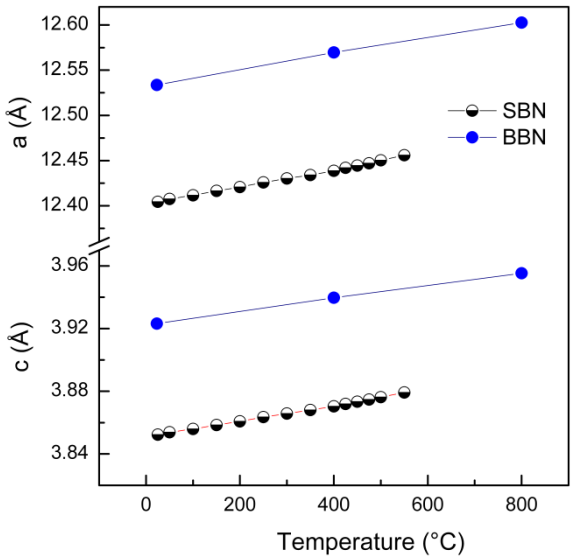

Fig. S6 Plots of the corresponding lattice parameters versus temperature for BBN and SBN. The patterns were fitted by Lebail fitting method using Fullprof software. The thermal expansion coefficient, determined from the unit cell volumes at the temperatures for BBN was $\bar{\alpha}_l = 8.3(1) \times 10^{-6} K^{-1}$.

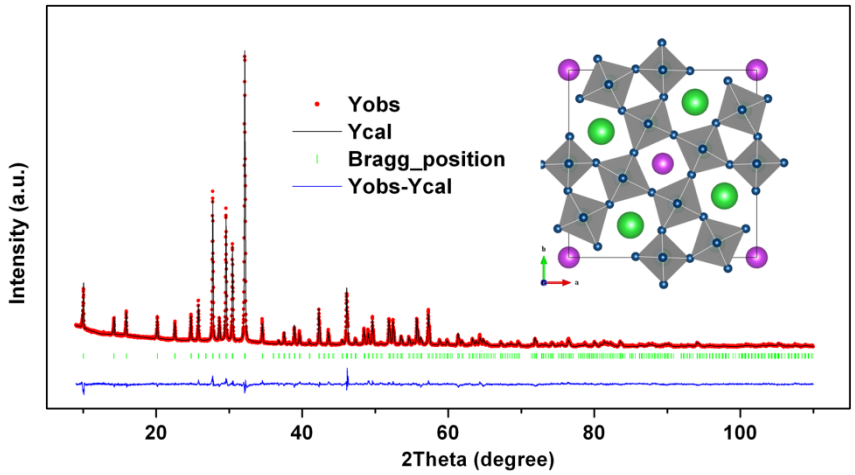

Fig S7 Rietveld refinement of the powder XRD pattern of BBNT collected at RT with space group P4bm using Fullprof software. Inset of the figure shows that Bi atoms are distributed in A1 sites, and Ba atoms remain in A2 sites respectively according to the refinement. There's no cationic vacancy in A site. The final reliability factors R_{wp} ~5.05% and R_p ~3.69%.

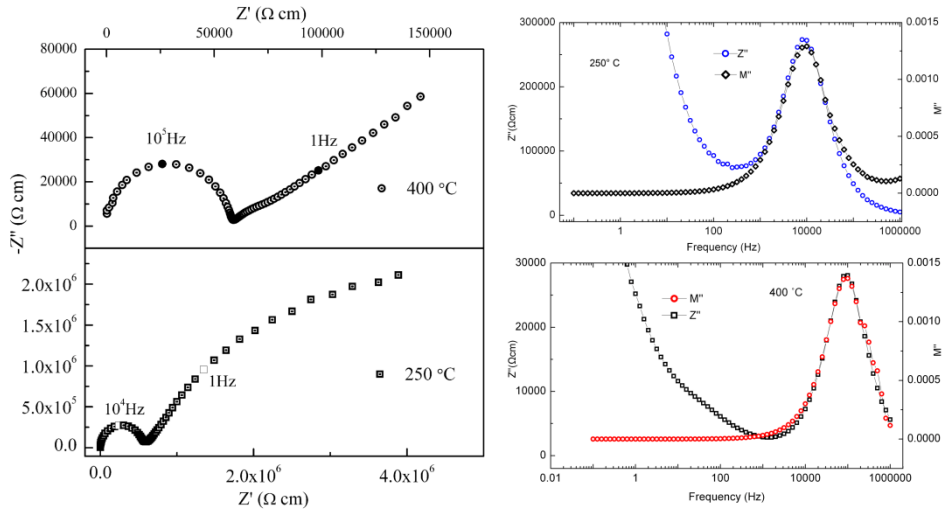

Fig S7 Left shows complex impedance plots for the BBN measured in air at 250°C and 400 °C in the range of 0.1Hz – 1MHz. Right shows Z''/M'' spectroscopic plots at 250°C and 400 °C for BBN sintered for 2 h.

The capacitances calculated from the semicircle in the high frequency range were 28.6 pF/cm and 31.8 pF/cm at 250°C and 400 °C, respectively The spike corresponding to Warburg electrode response was observed in these plots. The maxima of M'' spectra are dominated by components

with smallest capacitance corresponds to the bulk contribution. The contribution of grain boundary seems not obvious in the range of 250–600 °C. The Z'' and M'' curves almost overlapped into single peak indicating that the sample may be electrically homogeneous in the temperature range.

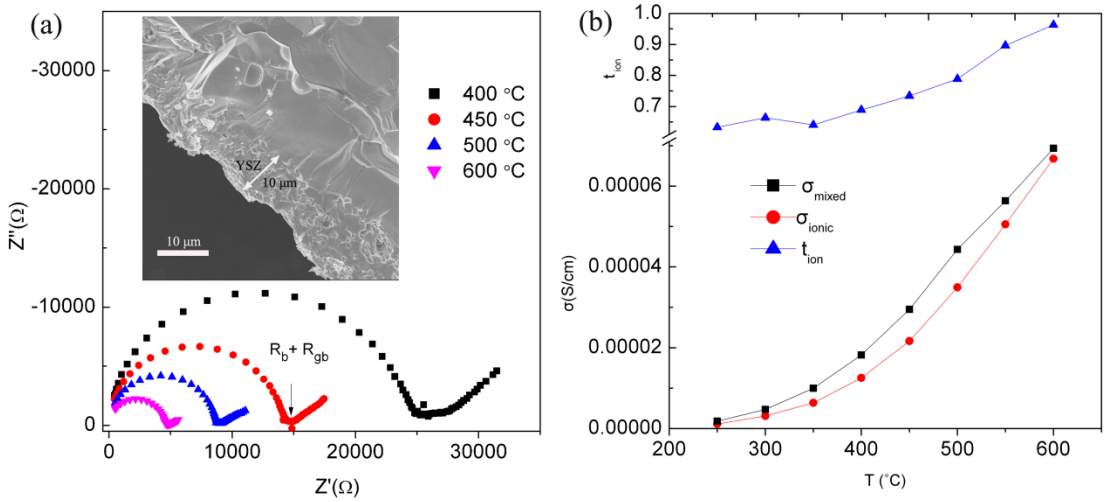

Fig. S8 (a) Complex impedance plots for YSZ-coated BBN, and SEM micrograph on the fracture surface before Ag coating. (b) Ionic transport number and conductivity vs Temperature.

To measure the ionic conductivity, we adopted a two-terminal blocking electrode method.[12] Both sides of the sintered pellets (~2 mm thickness) were sprayed with nano-YSZ (8 mole percent, particle size ~100 nm). After the spray the pellets was sintered at 1200 °C for 2 h, which formed a thin and dense layer (~10 μm) as electron blocking electrode(see **Fig S8**), then silver paste was coated. The resistance of the YSZ films was ignored as the resistivity and thickness is much smaller than the BBN pellets. The conductivities of the pellet with blocking electrodes were obtained from the impedance data measured from 250 °C to 600 °C, which is equal to the ionic conductivity (σ_{ionic}) as YSZ is considered to be almost a pure oxygen ion conductor.[3] The ionic transport number could be obtained by the relation $t_{ion} = \sigma_{ionic}/\sigma_{mixed}$ (**Fig. S8**), where σ_{mixed} is obtained from the primary sample (sintered at 1200°C for 2 h again). The t_{ion} was evaluated to be 0.66-0.94 with the temperature increasing from 250-600 °C in air.

[1] C. C. Chen, M. M. Nasrallah, H. U. Anderson, *J. Electrochem. Soc.*, 1995, **142**, 491–496.
[2] X. Li, H. Zhao, F. Gao, Z. Zhu, N. Chen , W. Shen, *Solid State Ionics*, 2008, **179**,1588–1592.
[3] D. J. L. Brett, A. Atkinson, N. P. Brandon and S. J. Skinner, *Chem. Soc. Rev.*, 2008, **37**, 1568–1578.

Table S1 Local and average compositions measured by EDS for BBN sintered for 2hours. The data were collected on 9 randomly selected areas and the standard errors were also listed.

Area No.	Nb (Atom%)	Ba (Atom%)	Bi (Atom%)
1	69.53(±1.92)	14.23(±1.37)	16.24(±1.83)
2	70.93(±2.03)	14.68 (±1.55)	14.39 (±2.06)
3	70.99(±1.90)	14.88(±1.34)	14.13(±1.80)
4	70.15(±2.22)	16.37(±2.93)	13.47(±2.21)
5	72.45(±1.99)	14.43(±1.41)	13.11(±1.87)
6	68.05(±2.07)	15.97(±2.59)	15.98(±2.11)
7	70.55(±4.46)	14.48(±3.08)	14.97(±2.70)
8	69.09(±1.97)	16.34(±1.43)	14.57(±1.87)
9	71.38(±2.28)	15.68(±3.01)	12.95(±2.27)
Average	70.35(±2.31)	15.23(±2.08)	14.42(±2.08)

Table S2 Selected Bond Lengths of Cations in A Sites for BBN at RT.

Atom 1-Atom 2	Distance (Å)	Atom 1-Atom 2	Distance (Å)
Bi1-O3 × 8	2.789(5)	Bi2a-O4 × 2	2.270(7)
Bi1-O5 × 4	2.722(7)	Bi2b-O2× 2	2.342(12)
Bi2-O1	3.41(3)	Bi2b-O3× 4	3.226(18)
Bi2-O2 × 2	2.925(18)	Bi2b-O4× 4	3.333(18)
Bi2-O3 × 2	2.49(2)	Bi2b-O5	2.67(2)
Bi2-O4 × 2	2.649(19)	Ba2-O1	3.077(3)
Bi2-O5	2.51(3)	Ba2-O2 × 2	2.789(5)
Bi2-O5	2.47(3)	Ba2-O3 × 4	3.301(6)
Bi2a-O1	2.561(13)	Ba2-O4 × 4	2.883(5)
Bi2a-O2 × 2	3.364(11)	Ba2-O5 × 2	3.460(8)
Bi2a-O3 × 2	2.967(11)	Ba2-O5 × 2	3.187(9)
Bi2a-O4 × 2	3.056(11)		